Eur. Phys. J. D **20**, 531–542 (2002)
DOI: 10.1140/epjd/e2002-00150-y

THE EUROPEAN PHYSICAL JOURNAL D

Exploration of the full conformational space of N-acetyl-L-glutamate-N-methylamide*

An ab initio and DFT study

M.F. Masman[1], M.A. Zamora[1,a], A.M. Rodríguez[1], N.G. Fidanza[2], N.M. Peruchena[2], R.D. Enriz[1], and I.G. Csizmadia[3]

[1] Departamento de Química, Universidad Nacional de San Luis, Chacabuco 915, 5700 San Luis, Argentina
[2] Area de Química Física, Departamento de Química, U.N.N.E., Av. Libertad 5460, 3400 Corrientes, Argentina
[3] Department of Chemistry, University of Toronto, Toronto, Ont., Canada M5S 3H6

Received 9 January 2002
Published online 13 September 2002 –

Abstract. A conformational and electronic study on N-acetyl-L-glutamate-N-methylamide was carried out. Theoretical computational analysis revealed 21 different conformations at the RB3LYP/6-31G(d) level of theory. *Ab initio* calculations at two levels of theory (RHF/3-21G and RHF/6-31G(d)) were also performed. All side-chain conformations were explored for this compound. N-acetyl-L-glutamate-N-methylamide displayed a different conformational behaviour in comparison with other amino acids possessing shorter side-chains. These results can be attributed, at least in part, to the side-chain-backbone interactions, which are stabilizing the low-energy conformations in this molecule.

PACS. 31.15.Ar Ab initio calculations – 31.15.Ew Density-functional theory

1 Introduction

A great deal of attention has been paid during the past several decades to the question of backbone folding in polypeptides. This is not surprising, as that is the main road towards the understanding of protein folding.

The conformational consequences of genetic engineering are seldom predictable. The relative orientation of the consecutive amide linkages (peptide bonds) determines the global fold. The exponentially growing number of conformers found in various protein databanks, accessible worldwide, has initiated new sub-fields and are emerging scientific areas of their own accord. New generations of structure prediction algorithms or alternative neural network analysis signal this trend. Although important, relative to those topics, the application of quantum mechanics for the analysis of peptides and protein fragments is less popular. This theoretical approach, although now accepted, still suffers from some skepticism. One of the most commonly asked questions is "Why calculate, if one can measure?". Due to the intrinsic flexibility of fragments of peptides and proteins measuring a single conformer by any spectroscopic method is often not straightforward. Very often NMR results need to be analyzed with the background knowledge of all topologically probable structures, perhaps determined by computation. In contrast to NMR, other branches of spectroscopy, with faster timescales, such as CD, UV and FTIR, reflect the sum of all energetically accessible forms. To understand and to interpret these spectra, they have to be deconvoluted and once again geometrical information could be essential. To help these analyses, calculated conformers are of great help.

A second inquiry could be stated: "Why perform expensive *ab initio* calculation instead of applying only a commonly used force-field?". Obviously, if we stick to the state of the art approach, the size and not the type of the molecule will predetermine the method to be used. A large variety of force-fields have been introduced in the past for the conformational analyses of peptides and proteins. From time to time, comparisons are published [1–3] to demonstrate their full capacity. Some of these force-field (HYPERCHEM [4], MM+ [5], AMBER [6], CHARMM [7] and OPLS [8,9]), along with the common semi-empirical MO approaches (MNDO/3 [10], MNDO [11], AM1 [12] and PM3 [13]) have been widely used to investigate molecules too large for *ab initio* studies. However, at least in the case of small peptides, these results are often much different from each other and from *ab initio* data [1–3].

Their inconsistency can be traced to the variation of the ordering of the relative energies for the same set of conformers, with different structural values. Furthermore, even the number of the allowed conformers varies from one method to another.

* Figures A_1–A_7 and Tables A–C are only available in electronic form at `http://www.edpsciences.org`

[a] e-mail: `mzamora@unsl.edu.ar`

The third most frequent objection against a theoretically determined structure library is "Why try to calculate all possible conformers, if they are not readily energetically accessible?". First of all, when the identification of the global minimum is the sole focus, often a large number of conformers are determined as "byproducts" of the protocol. Even if these "high energy" zero-gradient structures have low probability, they are not useless. They could be used as guides to understand basic questions such as the following. A protein can occupy its global minimum or one of its local minima, energetically not much higher than the global. Therefore, instead of discarding the so-called "high energy" structures, it is wiser to collect as many of these as possible.

The interaction between side-chain and backbone in peptides is a fundamental question that has not been answered satisfactorily as yet. Side-chain folding is not only interesting but also important because side-chain orientation can influence backbone folding *via* side-chain–backbone (SC/BB) interaction. Of course, the analysis of the phenomenon of side-chain folding requires relatively long aliphatic side-chains and there are only a handful of amino acids that fulfill the requirement. Glutamate has a long enough side-chain and is therefore a good candidate for the exploration of this conformational problem. Of the 20 naturally occurring amino acids there are only two amino acids, aspartic acid (Asp) and glutamic acid (Glu), which have carboxylic acid moieties in their side chains. Under biological conditions, they can deprotonate easily, forming a negatively charged side-chain. Such side-chains can be involved in salt-bridge [14] formation as illustrated by Structure 1.

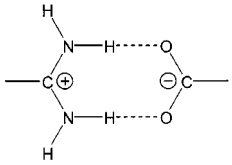

Structure 1.

Carboxylate ions may also form salts with metal cations. Calmoludin and other Ca^{2+} carrying proteins have a rather high proportion of glutamate, to bind Ca^{2+} ion, in addition to aspartate residues [15].

Both aspartate [16] and glutamate [17] residues have been studied previously, in an exploratory fashion. However, the present paper is the first in which the full conformational space of glutamate is explored.

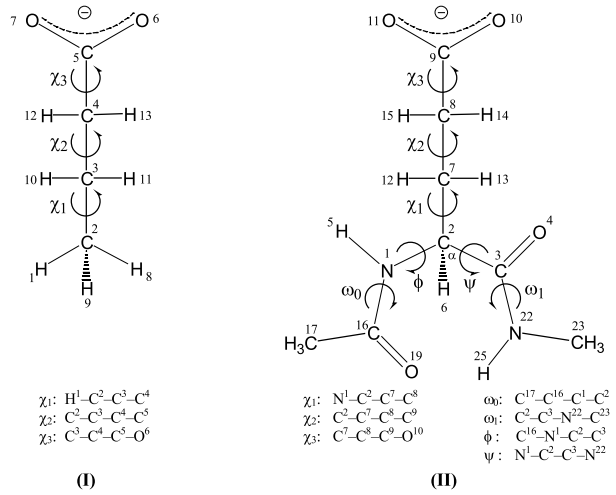

Figure 1. Numbering of the atoms and torsional angles for butyrate ion (I) and N-acetyl-L-glutamate-N-methylamide (II). The torsional angles are defined in terms of the atoms involved.

Due to the rather large dipole moment of an amide plane, it is obvious that a charged side-chain may have a backbone conformation influencing capacity. Clearly, a deeper understanding of these topics could be enhanced by explicit knowledge of the quantum mechanical conformational properties of N-acetyl-L-glutamate-N-methylamide (Fig. 1). We report here an exhaustive conformational and electronic study of N-acetyl-L-glutamate-N-methylamide using different levels of theory. A comparative study amongst theoretical calculations and experimental (NMR and X-ray) results was also carried out.

2 Methods

IUPAC-IUB [18] rules recommended the use of $0° \rightarrow +180°$ in clockwise direction (clockwise rotation) and $0° \rightarrow -180°$ for counter-clockwise direction (Scheme 1), for rotational potential. For side-chain rotation, this implied the following range: $-180° \leq \chi_1 \leq 180°$, $-180° \leq \chi_2 \leq 180°$ and $-180° \leq \chi_3 \leq 180°$. On the Ramachandran map (Scheme 2), the central box denoted by a broken line ($-180° \leq \phi \leq 180°$ and $-180° \leq \psi \leq 180°$) represents the cut suggested by the IUPAC convention. The four quadrants denoted by solid lines are the conventional or traditional cuts.

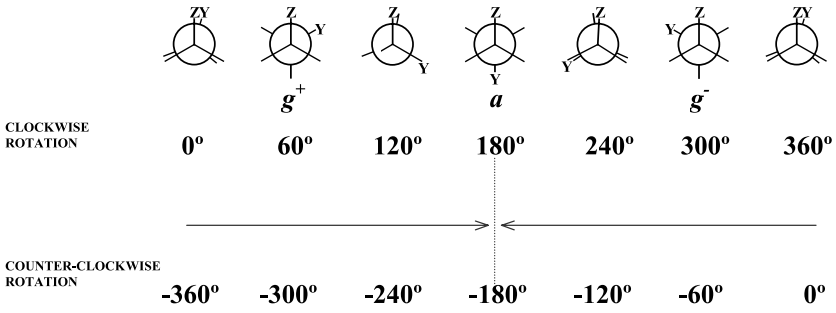

Scheme 1.

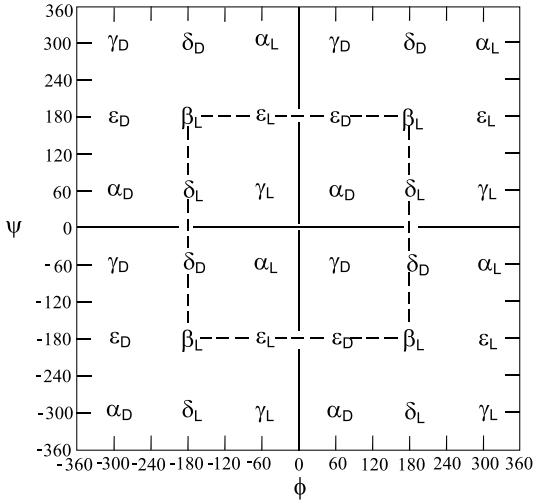

Scheme 2.

Most peptide residues exhibit nine unique conformations, labeled as α_{D} (α_{LEFT}), ε_{D}, γ_{D} (C_7^{ax}), δ_{L} (β_2), β_{L} (C_5), δ_{D} (α'), γ_{L} (C_7^{eq}), ε_{L}, and α_{L} (α_{RIGHT}).

However, for graphical presentation of the side-chain conformational potential energy surface (PES), we use the traditional cut ($0° \leq \chi_1 \leq 360°$ and $0° \leq \chi_2 \leq 360°$), similar to that suggested previously by Ramachandran and Sasisekharan [19].

2.1 Computations of molecular conformers

Molecular Geometry optimizations were performed at three levels of theory: RHF/3-21G, RHF/6-31G(d) and RB3LYP/6-31G(d), using the Gaussian 98 [20] program. Exploratory computations were first performed on the butyrate ion (I), at the RHF/3-21G level of theory, prior to the subsequent study carried out on N-acetyl-L-glutamate-N-methylamide (II). The numbering of the atoms together with the torsional angles, which were varied in both cases, is shown in Figure 1.

Features of the potential energy hypersurface (PEHS) (Eq. (1)) associated with the butyrate ion are shown as two potential energy surface (PES) cross-sections (Eqs. (2a, 2b)) in Figure 2

$$E = E\,(\chi_1, \chi_2, \chi_3), \tag{1}$$

$$E = E\,(\chi_1, \chi_2), \tag{2a}$$

$$E = E\,(\chi_2, \chi_3). \tag{2b}$$

These surfaces already revealed a $3 \times 3 \times 2$ topological periodicity along χ_1, χ_2 and χ_3 respectively, leading to 18 minima on the PEHS (Eq. (1)) where χ_3 assumed 0° and 180° orientations. These minima were optimized, revealing that each of 12 degenerate minima turned out to be the global energy minimum while each of the remaining 6 degenerate minima were observed to be the higher energy minimum. A table showing the optimized torsional angles, total energy values and relative energies for the conformational minima of butyrate ion (I) is available on the Web (Tab. A).

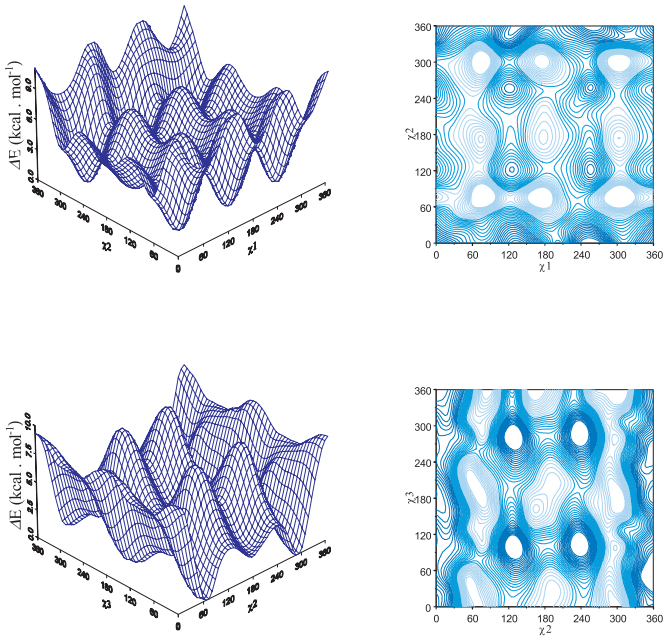

Figure 2. Conformational PES (landscape and contour map) for butyrate ion (I). Top: $E = E(\chi_1, \chi_2)$. Bottom: $E = E(\chi_2, \chi_3)$.

It was surprising to see that χ_3 did not have a minimum energy point at 90°, as it is often the case when a planar moiety is rotated about a tetrahedral moiety [21]. However, such minima might be expected to occur in the case of the glutamate residue since it is a more complex structure than butyrate. It seemed reasonable therefore to ignore χ_3 as a systematic variable. In view of that, one expects to see 9 backbone and 9 side-chain orientations, all together 81 conformers, each of which will have at least one optimum χ_3 value.

2.2 Stabilization energies

The stabilization energies were calculated with respect to the γ_{L} (C_7) as well as to the β_{L} (C_5) backbone conformation of N- and C-protected glycine [22,23] using the following isodesmic (same number of the same type of bonds) reaction, where the terminating groups P and Q are CH_3 and side-chain R = CH_2–CH_2–COO(–):

$$\underset{\text{reference conformation } \gamma_{\mathrm{L}} \text{ or } \beta_{\mathrm{L}}}{\mathrm{PCONH\text{–}CH_2\text{–}CONHQ} + \mathrm{CH_3\text{–}R}} \rightarrow \underset{\text{conformation X}}{\mathrm{PCONH\text{–}CHR\text{–}CONHQ}} + \mathrm{CH_3\text{–}H}.$$

The stabilization energy may be calculated as follows:

$$\begin{aligned}\Delta E_{\text{stabilization}} = \{&E[\mathrm{PCONH\text{–}CHR\text{–}CONHQ}]_{\mathrm{X}} \\ &+ E[\mathrm{CH_3\text{–}H}]\} \\ -\{&E[\mathrm{PCONH\text{–}CH_2\text{–}CONHQ}]_{\gamma_{\mathrm{L}} \text{ or } \beta_{\mathrm{L}}} \\ &+ E[\mathrm{CH_3\text{–}R}]\}\end{aligned}$$

Table 1. Total energy values of the component molecules for isodesmic reaction computed at three levels of theory.

		Energy (Hartree)		
Molecular System		**HF/3-21G**	**HF/6-31G(d)**	**B3LYP/6-31G(d)**
P–CONH–CH_2–CONH–**Q**	γ_L	**P = Q =** Me	**P = Q =** Me	**P = Q =** Me
		-451.294243	-453.823750	-456.537516
	β_L	**P = Q =** Me	**P = Q =** Me	**P = Q =** Me
		-451.293188	-453.824111	-456.536165
CH_3–**R**		**R =** CH_2–CH_2–$COO^{(-)}$	**R =** CH_2–CH_2–$COO^{(-)}$	**R =** CH_2–CH_2–$COO^{(-)}$
		-303.581790	-305.298474	-307.131563
		R = H	**R =** H	**R =** H
		-39.976877	-40.195167	-40.518389

The components' energy values are summarized in Table 1.

2.3 Topological analysis of electron density

The topology of the electron density has been analyzed using the AIM (atoms in molecules) method [24]. In this analysis, the gradient $[\nabla\rho(r)]$ and the Laplacian $[\nabla^2\rho(r)]$ play important roles. A critical point of the electron density along the line of two interacting atoms in a molecule is called the bond critical point (BCP), where $\nabla\rho(r) = 0$.

The bond path is made up of a pair of gradient paths, originating at a BCP and terminating at the neighbouring nuclei. The necessary condition for two atoms to be bonded to each other is that their nuclei must be linked by a bond path. The bond path is regarded to be "a universal indicator of bonded interaction" [25]. The method is widely used for the proof of existence of hydrogen bonds [26].

3 Results and discussion

3.1 Conformational study

The DFT results of the geometry optimizations of the title compound at the RB3LYP/6-31G(d) level of theory, including geometrical parameters, total energies, relative energies and stabilization energies are given in Table 2. The total energies are given in Hartree, the relative energies and stabilization energies are given in kcal mol^{-1} (using the conversion factor: 1 Hartree = 627.5095 kcal mol^{-1}). The same data obtained from *ab initio* calculations at the RHF/3-21G and RHF/6-31G(d) levels of theory are available on the Web (Tabs. B and C). While 21 relaxed structures were obtained from DFT calculations, 27 and 32 were obtained from *ab initio* RHF/6-31G(d) and RHF/3-21G levels of theory, respectively.

Side-chain PESs associated with each of the seven backbone conformations (no δ_L or δ_D backbone conformers were located) are shown in Figure 3 in which χ_3 was relaxed. The variation of χ_3 in the case of the α_D backbone as a function of χ_1 and χ_2 is shown in Figure 4.

The reliability of the RHF/3-21G level of computations can be investigated here since we have results from the RHF/6-31G(d) and RB3LYP/6-31G(d) levels. It is prudent, at this time, to make a comparison.

The relative energies (ΔE_{rel}) of the title compound, computed at three levels of theory, are compared in Figure 5. Since the global minimum, on the relative energy scale, is always zero by definition, in order for the fitted line to pass over the origin, a $y = mx$ equation was fitted to the data points. While the slopes of the fitted lines are never unity, it is clear that the RHF/3-21G results reproduce the trend quite well.

In addition to relative stabilities, accuracy of the key torsional angles (in the present case, ϕ, ψ, χ_1, χ_2, ω_0 and ω_1) is of great importance. The correlation of the above torsional angles computed at three levels of theory for the title compound is shown in Figure 6. The least-square fit was of the type $y = mx + b$. Neither m is unity nor b is zero for the RHF/3-21G and RHF/6-31G(d) calculations. However, the fitted lines suggest a surprisingly good correlation.

Some minima were annihilated as the level of theory was increased. This is illustrated in Figure 7.

3.2 Stabilization energies

The stabilization exerted by the side-chain on the backbone is traditionally calculated [22,23] with respect to the global minimum *i.e.* the γ_L conformation. However, it has been noted recently [27] that during cis-trans isomerization, the γ_L conformation may disappear at least for some of the amino acids. In other words, the γ_L conformer does not exist as a minimum energy conformation on some of the cis-Ramachandran maps. For this reason, as an alternative backbone conformation, β_L has been selected for the calculation of stabilization energy (ΔE_{stabil}). The method of calculation, as outlined in the "Computational Methods" section, is the same, but instead of the γ_L conformation of glycine, the β_L conformation is chosen as the reference conformation. Such a new standard may be important in the future, when some *ab initio* peptide database will include both cis and trans peptides. Nevertheless, today, the ΔE_{stabil} (γ_L) values are more practical if we wish to make comparisons to previously reported values. Figure 8 compares ΔE_{stabil} (γ_L) values for the title compound.

Such a "spectrum" of side-chain stabilization is presented in Figure 9.

Table 2. Torsional angles and total energy values for backbone and side-chain conformers (no δ_L or δ_D backbone conformers were located) of $CH_3CONH–Glu^{(-)}–CONHCH_3$ optimized at RB3LYP/6-31G(d) level of theory. The calculated relative energies (ΔE_{rel})[c] and stabilization energies (ΔE_{stabil}) are also shown.

Final Geometry	χ_1 (1-2-7-8)	χ_2 (2-7-8-9)	χ_3 (7-8-9-10)	ω_6 (17-16-1-2)	ω_1 (2-3-22-23)	ϕ (16-1-2-3)	ψ (1-2-3-22)	Total Energy (Hartree)	ΔE_{rel} (kcal . mol^{-1})	ΔE_{stabil} (γ_L) (kcal . mol^{-1})	ΔE_{stabil} (β_L) (kcal . mol^{-1})
α_D (g$^-$, g$^-$)						Not found					
α_D (g$^-$, a)						Not found					
α_D (g$^-$, g$^+$)						Not found					
α_D (a, g$^-$)						Not found					
α_D (a, a)						Not found					
α_D (a, g$^+$)						Not found					
α_D (g$^+$, g$^-$)	-67.53	89.50	84.83	150.92	-170.11	66.44	31.51	-723.179110341	9.13	-17.66	-18.51
α_D (g$^+$, a)	-55.24	-163.21	-153.71	155.77	-170.03	59.53	38.44	-723.151097892	26.71	-0.08	-0.93
α_D (g$^+$, g$^+$)	-40.12	-47.28	-106.01	163.83	-169.91	59.60	36.42	-723.178534010	9.49	-17.30	-18.15
ε_D (g$^-$, g$^-$)	45.36	116.87	-38.96	-159.42	-178.34	48.61	-148.65	-723.169873648	14.93	-11.86	-12.71
ε_D (g$^-$, a)						Not found					
ε_D (g$^-$, g$^+$)						Not found					
ε_D (a, g$^-$)	-169.71	53.06	102.63	154.08	-179.65	72.40	157.98	-723.179002941	9.20	-17.59	-18.44
ε_D (a, a)						Not found					
ε_D (a, g$^+$)						Not found					
ε_D (g$^+$, g$^-$)						Not found					
ε_D (g$^+$, a)	-61.31	-164.50	-156.77	168.02	174.05	56.09	-128.56	-723.155639981	23.86	-2.93	-3.78
ε_D (g$^+$, g$^+$)	-104.30	-66.36	-177.77	-155.75	-174.52	66.86	176.14	-723.177332016	10.25	-16.54	-17.39
γ_D (g$^-$, g$^-$)						Not found					
γ_D (g$^-$, a)						Not found					
γ_D (g$^-$, g$^+$)						Not found					
γ_D (a, g$^-$)						Not found					
γ_D (a, a)	-169.54	155.12	153.92	166.21	180.00	75.03	-65.67	-723.156432452	23.36	-2.87	-3.70
γ_D (a, g$^+$)						Not found					
γ_D (g$^+$, g$^-$)	-69.66	57.89	-88.55	150.70	-179.70	72.35	-40.72	-723.183741648	6.22	-20.57	-21.41
γ_D (g$^+$, a)						Not found					
γ_D (g$^+$, g$^+$)	-39.74	-47.11	-109.31	162.03	-176.70	60.86	-33.89	-723.183364341	6.46	-20.33	-21.18
β_L (g$^-$, g$^-$)	71.36	114.37	150.12	172.14	178.26	-157.30	-157.80	-723.185873661	4.89	-21.90	-22.75
β_L (g$^-$, a)						Not found					
β_L (g$^-$, g$^+$)						Not found					
β_L (a, g$^-$)	175.55	56.26	108.23	176.36	177.59	-157.31	160.92	-723.190109127	2.26	-24.56	-25.41
β_L (a, a)	-172.32	163.76	162.44	173.45	169.51	-134.82	161.10	-723.162692366	19.43	-7.36	-8.20
β_L (a, g$^+$)						Not found					
β_L (g$^+$, g$^-$)						Not found					
β_L (g$^+$, a)						Not found					
β_L (g$^+$, g$^+$)	-117.61	-71.68	-164.91	173.99	179.72	-172.85	175.05	-723.187217897	4.04	-22.75	-23.59
γ_L (g$^-$, g$^-$)						Not found					
γ_L (g$^-$, a)						Not found					
γ_L (g$^-$, g$^+$)	54.79	-85.99	-140.20	-169.93	-179.97	-79.63	54.90	-723.191490581	1.36	-25.43	-26.28
γ_L (a, g$^-$)						Not found					
γ_L (a, a)	-165.58	157.53	159.83	-171.46	-172.89	-82.56	78.99	-723.161449907	20.21	-6.58	-7.43
γ_L (a, g$^+$)						Not found					
γ_L (g$^+$, g$^-$)	-56.06	87.28	152.75	-167.25	-75.63	-82.21	63.16	**-723.193661001**	**0.00**	**-26.96**	**-27.81**
γ_L (g$^+$, a)						Not found					
γ_L (g$^+$, g$^+$)						Not found					
ε_L (g$^-$, g$^-$)						Not found					
ε_L (g$^-$, a)						Not found					
ε_L (g$^-$, g$^+$)						Not found					
ε_L (a, g$^-$)						Not found					
ε_L (a, a)						Not found					
ε_L (a, g$^+$)						Not found					
ε_L (g$^+$, g$^-$)						Not found					
ε_L (g$^+$, a)	-61.06	-156.33	-152.48	170.11	172.21	-73.84	164.86	-723.161063309	20.46	-6.33	-7.18
ε_L (g$^+$, g$^+$)						Not found					
α_L (g$^-$, g$^-$)	23.75	59.99	-69.75	-178.96	-174.16	-112.97	-41.13	-723.192716994	0.59	-26.20	-27.05
α_L (g$^-$, a)						Not found					
α_L (g$^-$, g$^+$)	60.19	-84.04	34.66	-171.26	179.80	-92.62	-10.71	-723.189193278	2.80	-23.99	-24.83
α_L (a, g$^-$)						Not found					
α_L (a, a)	-169.82	161.44	154.51	-166.76	179.94	-70.96	-35.74	-723.156457973	23.35	-3.45	-4.29
α_L (a, g$^+$)						Not found					
α_L (g$^+$, g$^-$)	-56.73	87.27	155.52	-167.74	179.29	-87.57	-15.84	-723.189765110	2.44	-24.55	-25.19
α_L (g$^+$, a)						Not found					
α_L (g$^+$, g$^+$)						Not found					

[c] The global minimum corresponds to γ_L (g$^-$,g$^+$) conformation having -723.193661001 hartree total energy. This value is taken a reference value, corresponding to Relative Energy 0.00 kcal.mol^{-1}.

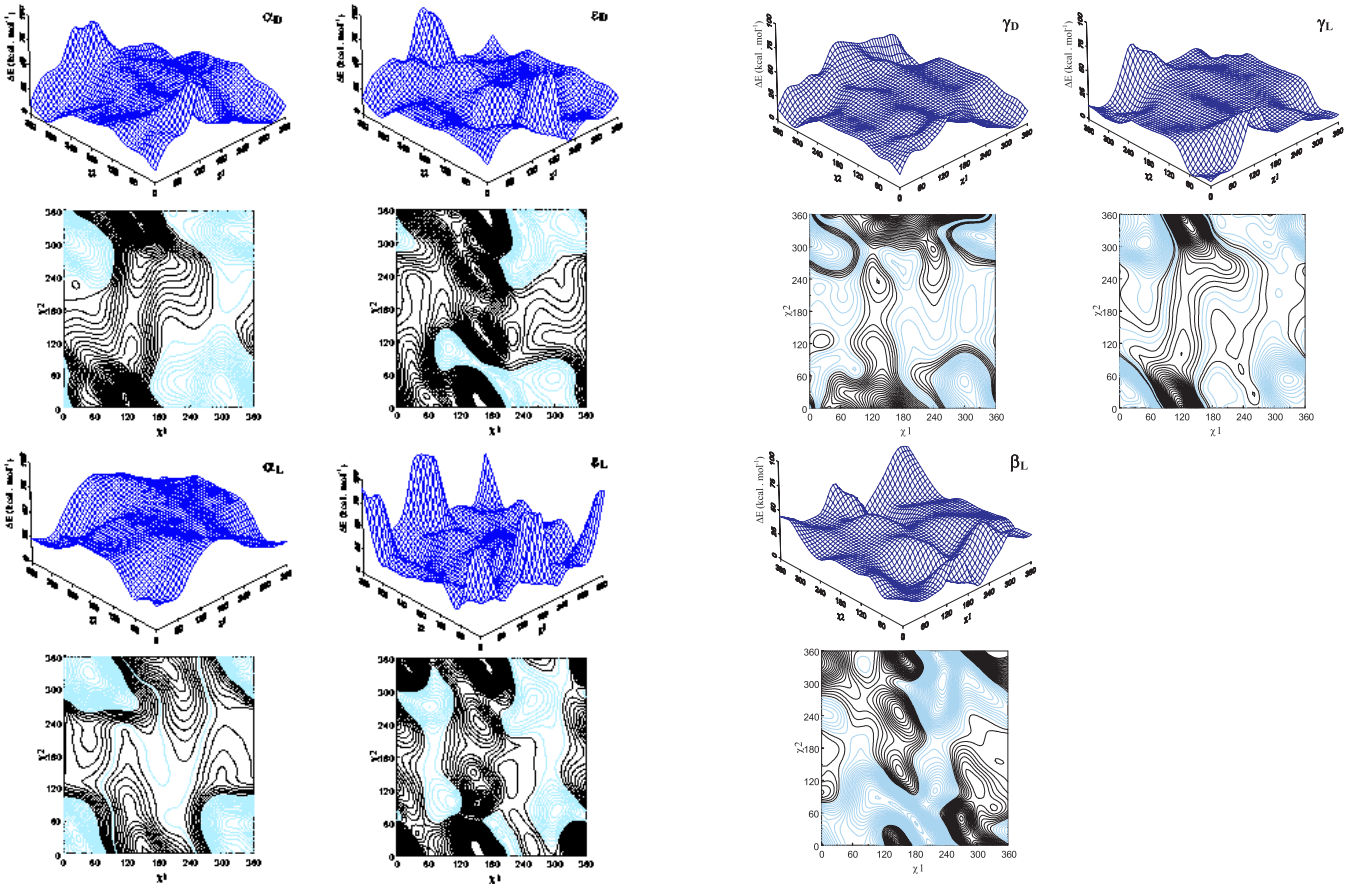

Figure 3. $E = E(\chi_1, \chi_2)$ PES for N-acetyl-L-glutamate-N-methylamide (II) in its seven different backbone conformations.

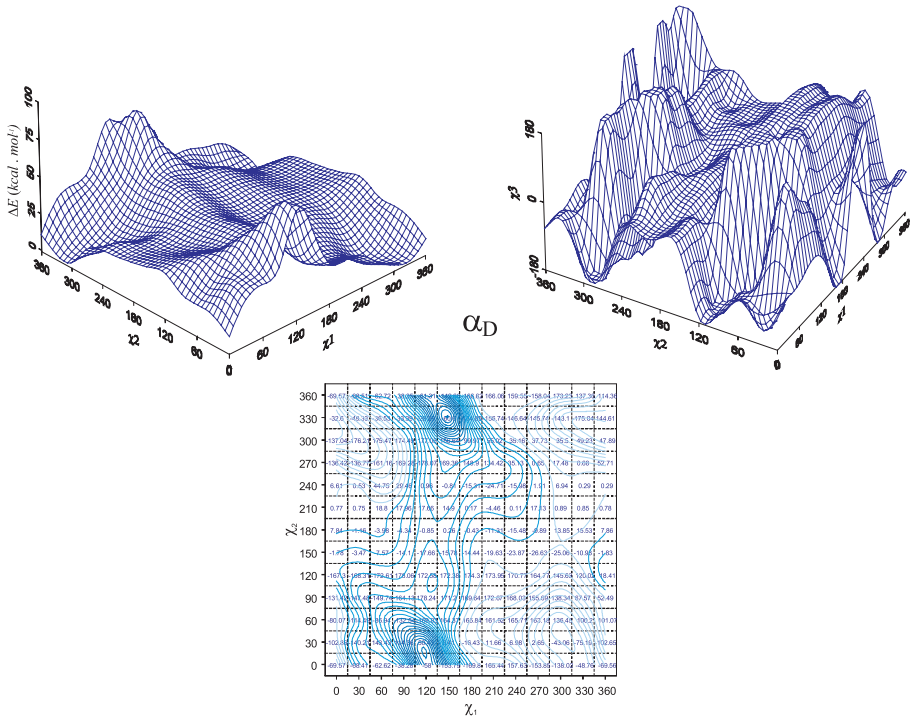

Figure 4. Potential energy surface landscape (top left) and contour map (bottom) associated with a fixed α_D backbone conformation for N-acetyl-L-glutamate-N-methylamide (II). In the contour map the values of χ_3 in each point was also included. The surface to the top right is showing the variation of χ_3 (between $-180°$ and $180°$) in function of χ_1 and χ_2.

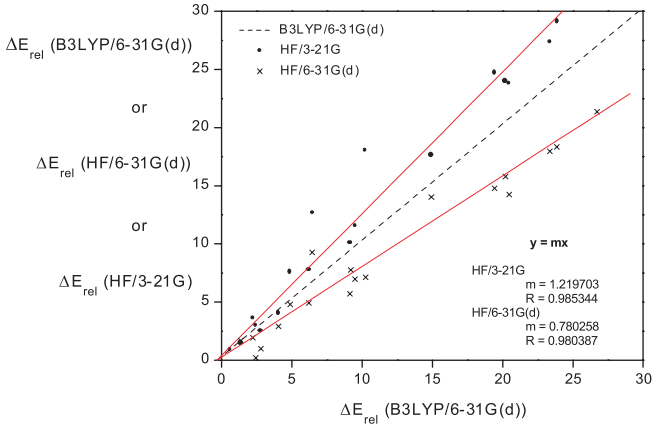

Figure 5. Correlation of relative energies computed at RB3LYP/6-31G(d), RHF/6-31G(d) and RHF/3-21G levels of theory for N-acetyl-L-glutamate-N-methylamide (II).

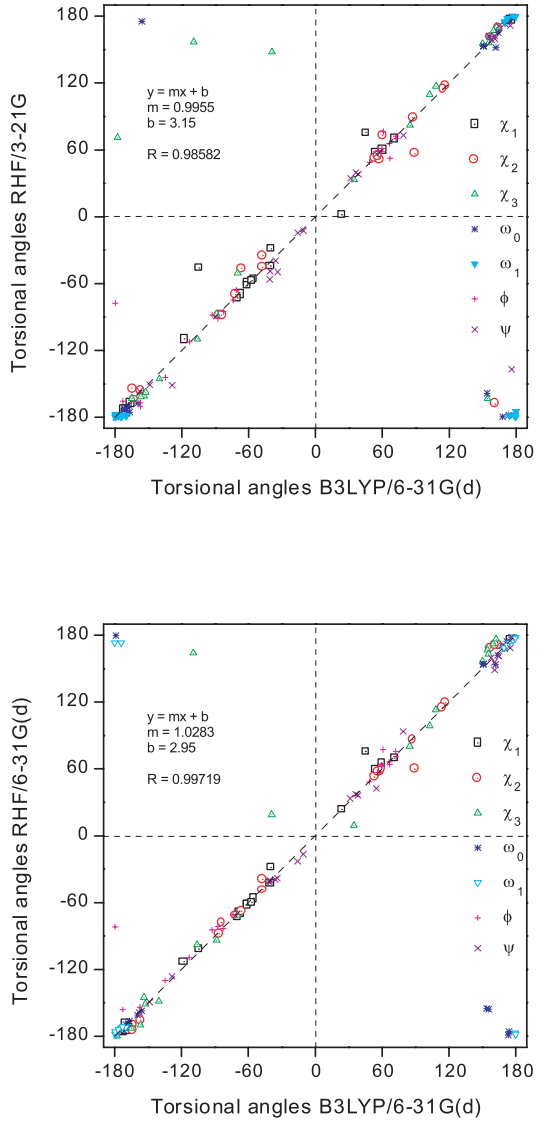

Figure 6. Correlation of torsional angles computed at RB3LYP/6-31G(d), RHF/6-31G(d) and RHF/3-21G levels of theory for N-acetyl-L-glutamate-N-methylamide (II).

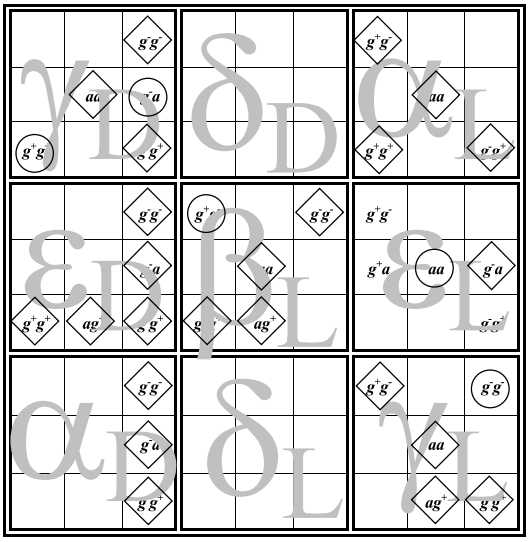

Figure 7. A schematic representation of the existing minima on the PEHS of four independent variables: $E = E(\phi, \psi, \chi_1, \chi_2)$ for N-acetyl-L-glutamate-N-methylamide (II). Bold letters: conformations obtained only at RHF/3-21G level of theory, ◯: conformations obtained at RHF/3-21G and RHF/6-31G(d) levels of theory, ◇: conformations obtained at the three levels of theory.

3.3 Intramolecular interactions

The two types of intramolecular hydrogen bonding (BB/BB; SC/BB) may occur in the various conformers of compound II, are depicted in Figure 10. The characteristic distances and angles as well as the classification of interactions are summarized in Table 3. Note that always the longer C–O of the carboxylate moiety is involved in the hydrogen bonding, acting as a proton acceptor (Tab. 4)

An AIM analysis revealed, in agreement with the data presented in Table 5, that extensive side-chain/backbone intermolecular hydrogen bonding type interaction exists in all backbone conformers.

Two representative structures showing hydrogen bonds as well as Molecular Electrostatic Potentials (MEPs), calculated with the PC SPARTAN PRO [28] software, are shown in Figure 11.

Computations have been carried out for the rest of the conformations, these figures are available on the Web (Figs. A_1–A_7)

In summary, different observations can be made with respect to the conformational and electronic intricacies of compound II:

(i) DFT calculations predict the existence of 21 conformations for compound II, being the $\gamma_L(g^-g^+)$ conformation the global minimum. This conformation possesses three internal hydrogen bonds, stabilizing its spatial ordering (Tab. 5);

(ii) the second global minimum is the $\alpha_L(g^+g^+)$ conformation. This is particularly noteworthy because

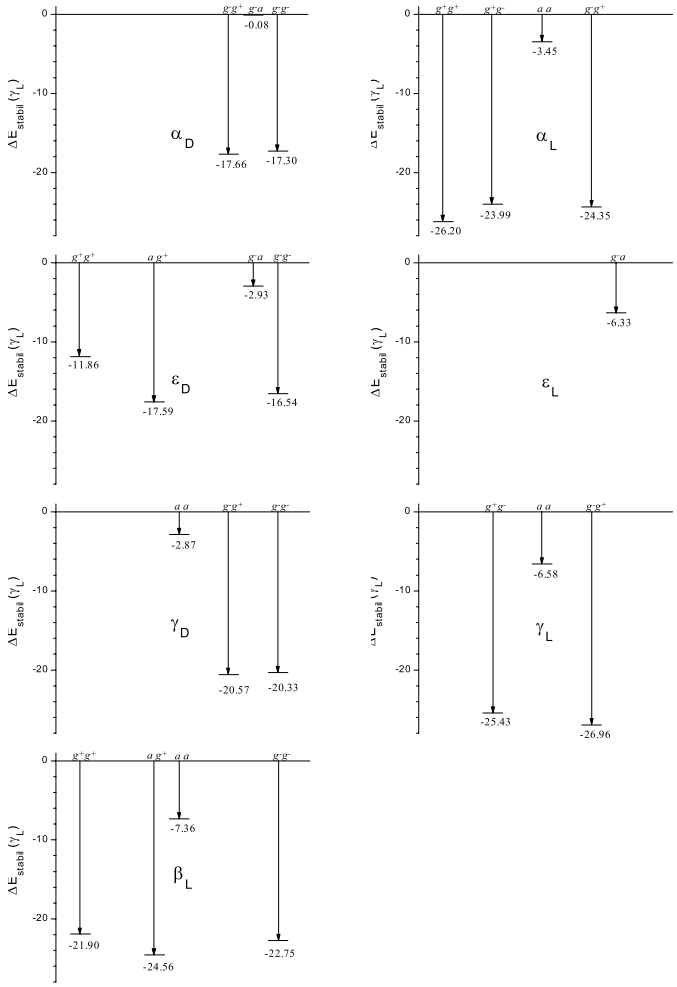

Figure 8. A graphical presentation of the ΔE_{stabil} (γ_{L}) values for all existing backbone and side-chain conformations of N-acetyl-L-glutamate-N-methylamide (II) at RB3LYP/6-31G(d) level of theory.

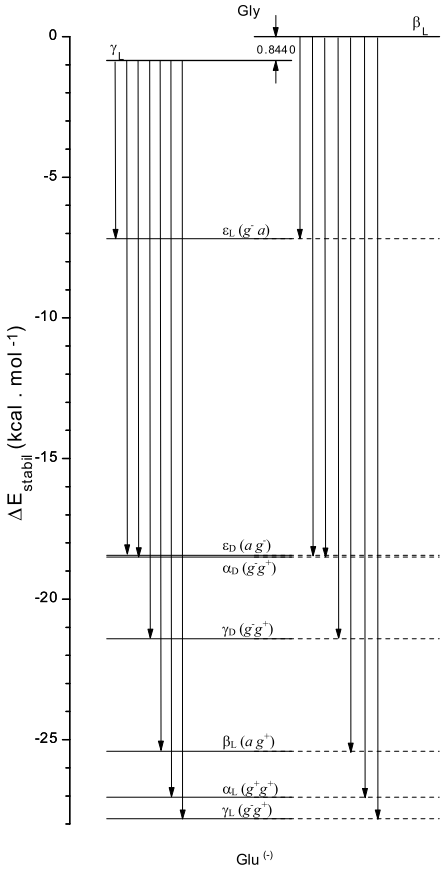

Figure 9. A graphical comparison for ΔE_{stabil} (γ_{L}) and ΔE_{stabil} (β_{L}) values for the minimum each backbone conformations of N-acetyl-L-glutamate-N-methylamide (II).

the α_{L} conformations are usually annihilated in other amino acids. This conformation display a particular spatial ordering, possessing a bifurcated hydrogen bond between N^{22}–$H^{25\cdots}O^{10}$ and N^{1}–$H^{5\cdots}O^{10}$ respectively (Fig. 11);

(iii) the α_{L} and ε_{L} conformations, which are usually annihilated, are now energy minima on the Ramachandran PES;

(iv) some other conformations (δ_{L} and δ_{D}), which are usually energy minima on the Ramachandran PES, now do not represent stable structures;

(v) Some backbone conformations do not tolerate the a, a side-chain orientations which is evident from the shifts observed.

Considering the conformational intricacies of compound II we can consider its conformational behavior as "non typical" if we compare the present results with those of other amino acids previously reported [29–32].

Table 3. Summary of intramolecular interactions in N-acetyl-L-glutamate-N-methylamide (II) optimized at RB3LYP/6-31G(d) level of theory.

Conformations	Interaction Type	Distance O···H (Å)	Angle N–H···O (Degrees)	$\Delta E_{\text{rel.}}$ (kcal . mol^{-1})
α_{D} (g^-, g^+)	2A	1.7925	149.75	9.13
α_{D} (g^-, g^-)	2A	1.6622	151.84	9.49
ε_{D} (g^+, g^+)	3B	1.6250	173.07	14.93
ε_{D} (a, g^+)	3A	1.6556	167.27	9.20
ε_{D} (g^-, g^-)	3A	1.6895	167.09	10.25
γ_{D} (a, a)	1A	1.9170	148.21	23.36
γ_{D} (g^-, g^+)	2B	1.8184	145.71	6.22
	1A	1.7566	159.04.	
γ_{D} (g^-, g^-)	2A	1.6401	154.15	6.46
	1A	1.7510	160.14	
β_{L} (g^+, g^+)	3A	1.6117	165.69	4.89
	1B	2.0590	112.12	
β_{L} (a, g^+)	3A	1.5866	169.13	2.23
	1B	2.0486	112.57	
β_{L} (a, a)	1B	2.1920	105.63	19.43
β_{L} (g^-, g^-)	3A	1.5916	172.55	4.04
	1B	2.0137	113.90	
γ_{L} (g^+, g^-)	2A	1.5193	171.46	1.36
	1A	1.8388	155.90	
γ_{L} (a, a)	1A	2.0292	144.88	20.21
γ_{L} (g^-, g^+)	**2A**	**1.5649**	**166.41**	**0.00**
	1A	**1.6771**	**154.77**	
α_{L} (g^+, g^+)	2B	1.7770	148.97	0.59
	3B	1.7820	161.47	
α_{L} (g^+, g^-)	2B	1.5677	169.03	2.80
α_{L} (g^-, g^+)	2A	1.5885	167.12	2.44

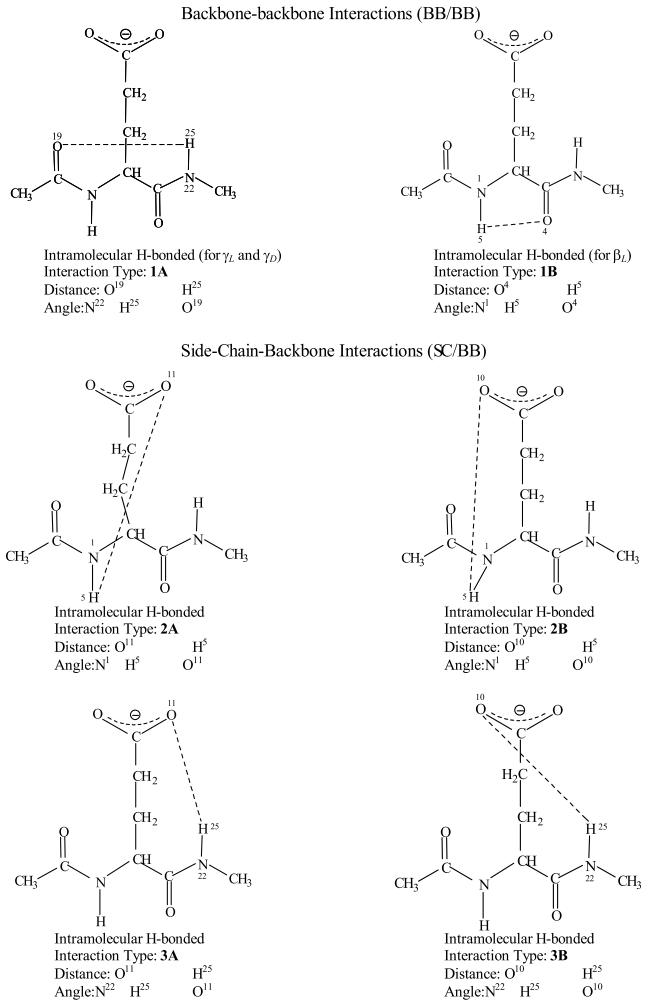

Figure 10. Classification of various types of backbone-backbone and side-chain-backbone interactions.

Table 4. Summary of C–O distances in carboxylate moiety in N-acetyl-L-glutamate-N-methylamide (II) optimized at RB3LYP/6-31G(d) level of theory.

Conformations	Interaction Type	C – O distance (Å)	
		involved in H–bond	not-involved
α_D (g^-, g^+)	2A	1.275	1.252
α_D (g^+, g^-)	2A	1.284	1.243
ε_D (g^+, g^+)	3B	1.283	1.242
ε_D (a, g^+)	3A	1.284	1.242
ε_D (g^-, g^-)	3A	1.276	1.244
γ_D (g^-, g^+)	2B	1.283	1.242
γ_D (g^+, g^-)	2A	1.284	1.241
β_L (g^+, g^+)	3A	1.282	1.241
β_L (a, g^+)	3A	1.284	1.240
β_L (g^-, g^-)	3A	1.279	1.243
γ_L (g^+, g^-)	2A	1.284	1.242
γ_L (g^-, g^+)	**2A**	**1.282**	**1.241**
α_L (g^+, g^+)	2B	1.293	1.238
	3B	1.293	1.238
α_L (g^+, g^-)	2B	1.280	1.243
α_L (g^-, g^+)	2A	1.281	1.241

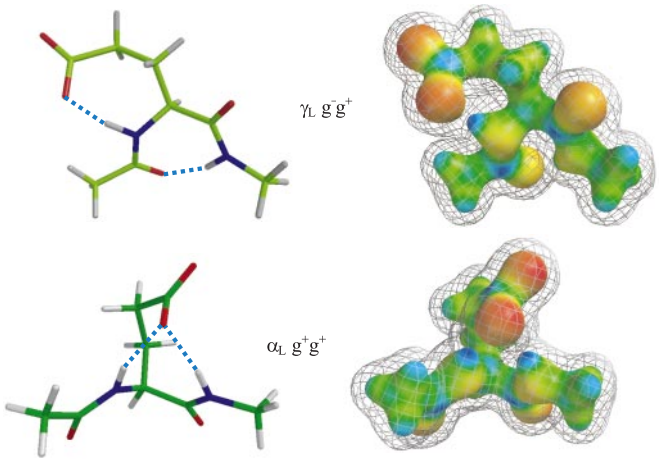

Figure 11. Two representative geometries showing hydrogen bonds calculated at RB3LYP/6-31G(d) and MEPs calculated at RHF/6-31G(d) levels of theory.

4 Correlation between natural occurrence of conformers and computed stability

To better understand the above theoretical results, we perform a comparison of structural parameters (torsional angles ϕ and ψ) from experimental data bases (X-ray and NMR) with our *ab initio* and DFT results. To keep the modeling as simple as possible it will be assumed that the probability of each conformer in proteins depends only on its relative energy. Obviously in this model several well-known phenomena are neglected, such as inter-residue interactions, long-range effects, hydration etc. However we believe that it is possible to correlate, in a simply way, the relative energy of a conformer and its relative probability in an ensemble of proteins. Thus the comparison of relative energies and the relative probabilities by using a non-homologous data base is a potential technique for the cross-validation of the two approaches.

Using a recent (February 2002) X-ray and NMR determined protein data set of non-homologous proteins [33], a population distribution map was generated. The backbone conformers of all 31159 Glu residues, found in a total of 974 non homologous proteins (99.2% TRANS and 0.8% CIS conformers), were plotted, showing ϕ against ψ values (Fig. 12a). To perform a comparison between calculated and observed backbone conformers, additional plots were made with the RHF/3-21G, RHF/6-31G(d) and RB3LYP/6-31G(d) results (Figs. 12b, 12c and 12d respectively).

Comparison of these data sets shows an overall promising similarity emerging. The experimental (X-ray and NMR) data indicate highly populated zones; the first one corresponds to the α_L (right-hand α-helix) and δ_D regions with 56.5% of the total population and the second is the β_L (extended β-strand), γ_L (inverse γ-turn), δ_L and ε_L regions with 40.6% of population. It is interesting to note that both *ab initio* and DFT calculations predict the γ_L (g^-g^+) and α_L (g^+g^+) as the energetically preferred conformers. These minima are distinguished in

Table 5. Topological properties at hydrogen bond critical points of $CH_3CONH–Glu^{(-)}–CONHCH_3$ minimum energy conformations. (RHF/6-311++G**//3-21G). Covalent bonds are denoted as X–H and hydrogen bonds specified as H···Y.

Conformers	Involved atoms	$\rho(r_c)$	$\nabla^2\rho(r_c)$	ε	λ_1	λ_2	λ_3	G	V	distance H···Y (Å)	angle X–H···Y (°)
α_D (g^-, g^-)	N^1–H^5···O^{11}	0.0368	0.1392	0.0913	-0.0524	-0.0480	0.2396	0.0344	-0.0340	1.798	143.2
	N^{22}–H^{25}···N^1	0.0188	0.0845	1.3289	-0.0185	-0.0079	0.1109	0.0179	-0.0147	2.257	107.3
	C^{17}–H^{20}···O^{10}	0.0145	0.0509	0.0938	-0.0153	-0.0140	0.0801	0.0112	-0.0096	2.251	144.7
α_D (g^-, g^-)	N^1–H^5···O^{11}	0.0518	0.1693	0.0273	-0.0892	-0.0868	0.3453	0.0484	-0.0545	1.657	145.8
ε_D (g^+, g^+)	N^{22}–H^{25}···O^{11}	0.0555	0.1621	0.0505	-0.1037	-0.0987	0.3645	0.0500	-0.0594	1.617	174.0
	C^8–H^{15}···O^{19}	0.0138	0.0497	0.0190	-0.0139	-0.0137	0.0773	0.0109	-0.0094	2.300	136.7
	C^7–H^{13}···O^{11}	0.0195	0.0896	6.0762	-0.0171	-0.0024	0.1091	0.0194	-0.0163	2.249	107.4
ε_D (a, g^+)	C^2–H^6···O^{11}	0.0180	0.0672	0.1231	-0.0179	-0.0159	0.1010	0.0150	-0.0131	2.233	119.1
	N^{22}–H^{25}···O^{11}	0.0521	0.1638	0.0394	-0.0934	-0.0899	0.3472	0.0480	-0.0550	1.646	162.2
	C^7–H^{12}···O^{19}	0.0150	0.0567	0.1234	-0.0149	-0.0132	0.0848	0.0124	-0.0107	2.316	116.8
	C^8–H^{15}···N^{22}	0.0108	0.0396	0.3302	-0.0078	-0.0058	0.0532	0.0084	-0.0069	2.615	107.3
ε_D (g^-, g^+)	N^1–H^5···O^{11}	0.0375	0.1475	0.0677	-0.0590	-0.0506	0.2521	0.0363	-0.0357	1.789	136.2
	C^7–H^{13}···O^{19}	0.0109	0.0423	0.3176	-0.0080	-0.0060	0.0563	0.0092	-0.0078	2.479	118.3
	C^7–H^{12}···N^{22}	0.0236	0.0563	0.6382	-0.0114	-0.0069	0.0746	0.0117	-0.0093	2.532	102.5
ε_D (g^-, a)	C^7–H^{12}···O^{11}	0.0222	0.0952	0.4479	-0.0234	-0.0161	0.1347	0.0207	-0.0176	2.141	110.2
	C^7–H^{13}···O^{19}	0.0099	0.0371	0.9610	-0.0081	-0.0042	0.0494	0.0081	-0.0070	2.565	112.6
ε_D (g^-, g^-)	N^{22}–H^{25}···O^{11}	0.0411	0.1511	0.0294	-0.0635	-0.0617	0.2764	0.0389	-0.0399	1.755	139.8
	C^2–H^6···O^{10}	0.0145	0.0584	1.8671	-0.0108	-0.0038	0.0731	0.0131	-0.0116	2.442	101.6
γ_D (g^+, g^+)	C^8–H^{15}···O^{19}	0.0131	0.0461	0.0632	-0.0131	-0.0123	0.0715	0.0102	-0.0089	2.329	140.0
	N^{22}–H^{25}···O^{19}	0.0245	0.1042	0.0810	-0.0329	-0.0304	0.1675	0.0231	-0.0202	1.956	145.1
	C^{23}–H^{24}···O^{11}	0.0115	0.0414	0.2539	-0.0113	-0.0090	0.0618	0.0091	-0.0078	2.399	124.8
γ_D (a, a)	C^7–H^{13}···O^{11}	0.0213	0.0918	0.5544	-0.0221	-0.0142	0.1281	0.0199	-0.0169	2.169	108.7
	C^7–H^{12}···O^{19}	0.0103	0.0371	0.2622	-0.0085	-0.0067	0.0524	0.0082	-0.0072	2.537	115.1
	N^{22}–H^{25}···O^{19}	0.0273	0.1144	0.0678	-0.0038	-0.0354	0.1877	0.0259	-0.0233	1.908	146.3
γ_D (g^-, g^+)	N^1–H^5···O^{10}	0.0338	0.1369	0.1237	-0.0461	-0.0410	0.2197	0.0317	-0.0302	1.842	136.7
	C^{17}–H^{20}···O^{11}	0.0158	0.0566	0.0972	-0.0170	-0.0155	0.0891	0.0123	-0.0106	2.111	143.7
	N^{22}–H^{25}···O^{19}	0.0396	0.1517	0.0550	-0.0645	-0.0611	0.2774	0.0384	-0.0389	1.749	155.8
γ_D (g^-, a)	N^{22}–H^{25}···O^{19}	0.0298	0.1239	0.0606	-0.0430	-0.0405	0.2074	0.0286	-0.0263	1.867	148.8
	C^7–H^{13}···O^{19}	0.0099	0.0361	0.3569	-0.0080	-0.0059	0.0500	0.0080	-0.0069	2.563	114.3
γ_D (g^-, g^-)	C^{17}–H^{20}···O^{10}	0.0140	0.0470	0.0482	-0.0138	-0.0132	0.0739	0.0103	-0.0089	2.273	153.4
	N^1–H^5···O^{11}	0.0168	0.0664	0.3378	-0.0150	-0.0112	0.0927	0.0149	-0.0131	2.139	119.3
	N^{22}–H^{25}···O^{19}	0.0354	0.1397	0.0587	-0.0552	-0.0522	0.2470	0.0340	-0.0332	1.795	155.2
	N^1–H^5···O^{10}	0.0203	0.0825	0.3485	-0.0193	-0.0143	0.1161	0.0179	-0.0153	3.078	108.8
β_L (g^+, g^+)	N^{22}–H^{25}···O^{11}	0.0572	0.1651	0.0497	-0.1074	-0.1023	0.3747	0.0515	-0.0618	1.605	166.1
	C^7–H^{13}···O^{11}	0.0197	0.0863	1.3085	-0.0177	-0.0077	0.1119	0.0188	-0.0160	2.242	107.8
	C^7–H^{12}···O^{19}	0.0120	0.0430	0.1856	-0.0110	-0.0093	0.0633	0.0095	-0.0083	2.422	121.7
	N^1–H^5···O^4	0.0245	0.1208	0.6309	-0.0262	-0.0160	0.1630	0.0258	-0.0213	2.045	111.5
β_L (g^+, g^-)	N^1–H^5···O^{10}	0.0276	0.1072	0.3460	-0.0358	-0.0266	0.1696	0.0245	-0.0221	1.933	144.8
	C^{17}–H^{20}···O^{10}	0.0110	0.0368	0.1108	-0.0106	-0.0096	0.0570	0.0082	-0.0071	2.844	107.3
β_L (a, g^+)	C^7–H^{13}···O^{19}	0.0085	0.0319	0.5558	-0.0066	-0.0043	0.0428	0.0070	-0.0060	2.607	117.0
	N^1–H^5···O^4	0.0251	0.1211	0.4951	-0.0284	-0.0190	0.1686	0.0260	-0.0218	2.027	112.8
	C^2–H^6···O^{11}	0.0154	0.0569	0.2077	-0.0145	-0.0120	0.0833	0.0127	-0.0112	2.340	111.8
	N^{22}–H^{25}···O^{11}	0.0594	0.1734	0.0331	-0.1128	-0.1092	0.3954	0.0545	-0.0657	1.591	162.8
	C^8–H^{15}···N^{22}	0.0103	0.0378	0.1938	-0.0068	-0.0057	0.0501	0.0080	-0.0066	2.646	105.6
β_L (a, a)	C^8–H^{14}···N^{22}	0.0100	0.0366	0.4072	-0.0068	-0.0048	0.0482	0.0077	-0.0062	2.711	105.4
β_L (g^-, g^-)	C^8–H^{14}···O^{19}	0.0090	0.0306	0.0510	-0.0081	-0.0077	0.0464	0.0068	-0.0059	2.531	131.9
	N^1–H^5···O^4	0.0251	0.1205	0.4564	-0.0286	-0.0196	0.1687	0.0259	-0.0217	2.027	112.7
	N^{22}–H^{25}···O^{11}	0.0528	0.1822	0.0242	-0.0950	-0.0928	0.3700	0.0522	-0.0588	1.608	163.6
	C^2–H^6···O^{11}	0.0147	0.0564	0.5116	-0.0132	-0.0087	0.0784	0.0127	-0.0122	2.401	105.3
γ_L (g^+, g^-)	N^{22}–H^{25}···O^{19}	0.0335	0.1322	0.1322	-0.0500	-0.0473	0.2296	0.2296	-0.0306	1.819	153.9
	C^8–H^{14}···O^4	0.0105	0.0407	0.0407	-0.0077	-0.0054	0.0538	0.0538	-0.0075	2.524	111.9
	N^1–H^5···O^{11}	0.0772	0.1834	0.0521	-0.1688	-0.1604	0.5125	0.0693	-0.0928	1.492	170.6
γ_L (a, g^+)	C^2–H^6···O^{11}	0.0223	0.0883	0.1609	-0.0261	-0.0224	0.1368	0.0195	-0.0169	2.090	125.4
	N^{22}–H^{25}···O^{19}	0.0229	0.0948	0.0762	-0.0294	-0.0273	0.1515	0.0210	-0.0182	1.992	143.0
γ_L (a, a)	C^7–H^{13}···O^{11}	0.0198	0.0887	0.0887	-0.0190	-0.0088	0.1165	0.0192	-0.0163	2.233	102.8
	N^{22}–H^{25}···O^{19}	0.0217	0.0895	0.0895	-0.0271	-0.0253	0.1419	0.0197	-0.0171	2.018	142.7
γ_L (g^-, g^+)	N^1–H^5···O^{11}	0.0682	0.1827	0.1827	-0.1382	-0.1325	0.4535	0.0624	-0.0790	1.541	164.1
	N^{22}–H^{25}···O^{19}	0.0310	0.1238	0.1238	-0.0451	-0.0425	0.2114	0.0292	-0.0274	1.852	152.7
γ_L (g^-, g^-)	N^{22}–H^{25}···O^{19}	0.0253	0.1049	0.0656	-0.0340	-0.0319	0.1708	0.0235	-0.0208	1.942	146.3
	C^2–H^6···O^{11}	0.0208	0.0812	0.1361	-0.0229	-0.0202	0.1243	0.0178	-0.0154	2.126	124.5
ε_L (g^+, a)	N^{22}–H^{25}···O^{11}	0.0496	0.1550	0.0539	-0.0881	-0.0836	0.3266	0.0449	-0.0511	1.661	169.3
	C^7–H^{13}···O^{11}	0.0200	0.0876	1.2648	-0.0183	-0.0081	0.1141	0.0191	-0.0162	2.229	108.6
ε_L (g^+, g^-)	N^1–H^5···O^{11}	0.0597	0.1740	0.0538	-0.0115	-0.0190	0.3989	0.0549	-0.0663	1.588	163.9
	C^8–H^{14}···O^4	0.0107	0.0387	0.7653	-0.0096	-0.0054	0.0537	0.0084	-0.0070	2.463	131.4
ε_L (a, a)	C^7–H^{13}···O^{11}	0.0194	0.0874	1.3800	-0.0185	-0.0078	0.1137	0.0189	-0.0160	2.245	102.7
ε_L (g^-, g^+)	N^1–H^5···O^{11}	0.0553	0.1718	0.0438	-0.1021	-0.0978	0.3717	0.0516	-0.0602	1.617	160.9
ε_L (g^-, a)	C^7–H^{12}···O^{11}	0.0221	0.0953	0.4861	-0.0233	-0.0157	0.1344	0.0207	-0.0176	2.145	109.6
α_L (g^+, g^+)	N^{22}–H^{25}···O^{10}	0.0393	0.1472	0.0375	-0.0616	-0.0594	0.2683	0.0377	-0.0386	1.742	163.2
	N^1–H^5···O^{10}	0.0473	0.1645	0.0511	-0.0795	-0.0756	0.3196	0.0450	-0.0489	1.694	149.5
α_L (g^+, g^-)	N^{22}–H^{25}···N^1	0.0202	0.0873	0.0873	-0.2030	-0.0120	0.1197	0.0188	-0.0157	2.217	108.8
	N^1–H^5···O^{10}	0.0675	0.1827	0.1827	-0.1383	-0.1308	0.4518	0.0620	-0.0782	1.541	167.1
α_L (a, a)	C^7–H^{12}···O^{11}	0.0197	0.0900	1.8046	-0.0184	-0.0065	0.1149	0.0195	-0.0166	2.250	100.6
α_L (g^-, g^+)	N^1–H^5···O^{11}	0.0647	0.1816	0.1816	-0.1275	-0.1225	0.4317	0.0597	-0.0740	1.560	164.1
	N^{22}–H^{25}···N^1	0.0208	0.0901	0.0901	-0.0214	-0.0132	0.1247	0.0194	-0.0163	2.197	109.2

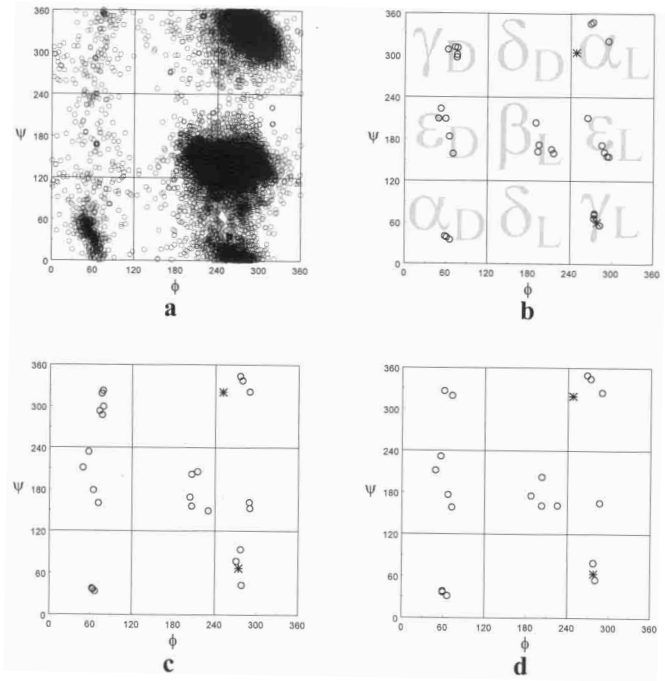

Figure 12. Backbone conformers of all 31159 Glu residues taken from 974 non homologous proteins [33]. Using their backbone dihedral parameters, all of the above Glu residues were plotted on a [ϕ, ψ] map (a). Locations of calculated compound II backbone conformers on a [ϕ, ψ] map obtained from: *ab initio* RHF/3-21G (b), RHF/6-31G(d) (c) and DFT (RB3LYP/6-31G(d)) (d) calculations. The two low-energy values obtained for the three levels of theory are shown with stars.

Figures 12b, 12c and 12d with stars. The α_D zone, which corresponds to the left-hand α-helix region, displays a moderate population (1.9%), whereas the γ_D and ε_D have a very low density with 0.5% and 0.4% respectively. Theoretical calculations predict these conformations as energetically disfavoured forms. From the results shown in Figure 12 it is clear that theoretical calculations are in complete agreement with experimental data. Such a correlation permits us to assume that if the amide model is relevant to the description of main chain folding of proteins, then the most stable conformers should have the lowest energy.

5 Conclusions

Multidimensional conformational analysis predicts 81 structures in the case of N-acetyl-L-glutamate-N-methylamide. Among these, 21 relaxed structures were determined at the DFT (RB3LYP/6-31G(d)) level of theory. The three levels of theory reported here (RHF/3-21G, RHF/6-31G(d) and RB3LYP/6-31G(d)) displayed closely related results indicating that RHF/3-21G calculations are sufficient to use in exploratory conformational analysis. The theoretical results are in good agreement with the experimental (X-ray and NMR) results.

Comparing the results obtained for N-acetyl-L-glutamate-N-methylamide with other previously reported amino acids, "atypical conformational behaviour" was obtained for this compound. Thus, the α_L and ε_L conformations which are usually annihilated are now stable energy minima on the Ramachandran PES, while δ_L and δ_D conformations which are usually energy minima for the rest of the amino acids, do not represent stable conformers for this system. This atypical behaviour might be attributed, at least in part, to the side-chain backbone interactions which occur in this molecule. This study can contribute to a better understanding of some less noticeable effects, which might strongly influence the structure of a polypeptide or a protein possessing this residue in their structures.

This work was supported by grants from Universidad Nacional de San Luis (UNSL), Universidad Nacional del Nordeste (UNNE), and Consejo Nacional de Investigaciones Científicas y Técnicas (CONICET) of Argentina. R.D.E. is a carreer researcher of CONICET. Authors want to express their acknowledgement to Dr. H.A. Baldoni for his help in making Figure 12.

References

1. I. Roterman, M. Lambert, K. Gibson, H. Scheraga, J. Biomol. Struct. Dyn. **7**, 421 (1989)
2. M. McAllister, A. Perczel, P. Császár, W. Viviani, J. Rivail, I. Csizmadia, J. Mol. Struct. (Theochem) **288**, 161 (1993)
3. A. Rodríguez, H. Baldoni, F. Suvire, R. Nieto-Vazquez, G. Zamarbide, R. Enriz, Ö. Farkas, A. Perczel, I. Csizmadia, J. Mol. Struct. (Theochem) **455**, 275 (1998)
4. HYPERCHEM 4.5, (1994) Hypercube, Inc. 419 Phillip St., Waterloo, Ontario, Canada N21, 3X2
5. N. Allinger, J. Am. Chem. Soc. **99**, 8127 (1977)
6. S. Wiener, U. Singh, T. O'Donnel, P. Kollman, J. Am. Chem. Soc. **106**, 6243 (1984)
7. B. Brooks, R. Bruccoleri, B. Olafson, D. States, S. Swaminathan, M. Karplus, J. Comp. Chem. **4**, 187 (1983)
8. W. Jorgensen, J. Tirado-Rives, J. Am. Chem. Soc. **110**, 1657 (1988)
9. J. Pranate, S. Wierschke, W. Jorgenson, J. Am. Chem. Soc. **113**, 2810 (1991)
10. R. Bringham, M. Dewar, D. Lo, J. Am. Chem. Soc. **97**, 1302 (1975)
11. M. Dewar, W. Thiel, J. Am. Chem. Soc. **99**, 4899 (1977)
12. M. Dewar, E. Zoebisch, E. Healy, J. Stewardt, J. Am. Chem. Soc. **107**, 3902 (1986)
13. J. Stewardt, J. Comp. Chem. **10**, 221 (1989)
14. Z. Székely, Z. Konya, A. Becskei, W.P.D. Goldring, A. Perczel, B. Penke, J. Molnár, C.J. Michejda, A. Aszalós, I.G. Csizmadia, J. Mol. Struct. (Theochem) **367**, 159 (1996)
15. M.R. Nelson, W.J. Chazin, BioMetals **11**, 297 (1998)
16. S.J. Salpietro, A. Perczel, Ö. Farkas, R.D. Enriz, I.G. Csizmadia, J. Mol. Struct. (Theochem) **497**, 39 (2000)
17. M.F. Masman, M.G. Amaya, A.M. Rodríguez, F.D. Suvire, G.A. Chasse, Ö. Farkas, A. Perczel, R.D. Enriz, J. Mol. Struct. (Theochem) **543**, 203 (2001)
18. IUPAC-IUB, Comission on Biochemical Nomenclature, Biochemistry **9**, 3471 (1970)

19. I. Ramachandran, V. Sasisekharan, Adv. Protein Chem. **23**, 283 (1968)
20. *Gaussian 98, Revision A.7*, M.J. Frisch, G.W. Trucks, H.B. Schlegel, G.E. Scuseria, M.A. Robb, J.R. Cheeseman, V.G. Zakrzewski, J.A. Montgomery Jr, R.E. Stratmann, J.C. Burant, S. Dapprich, J.M. Millam, A.D. Daniels, K.N. Kudin, M.C. Strain, O. Farkas, J. Tomasi, V. Barone, M. Cossi, R. Cammi, B. Mennucci, C. Pomelli, C. Adamo, S. Clifford, J. Ochterski, G.A. Petersson, P.Y. Ayala, Q. Cui, K. Morokuma, D.K. Malick, A.D. Rabuck, K. Raghavachari, J.B. Foresman, J. Cioslowski, J.V. Ortiz, A.G. Baboul, B.B. Stefanov, G. Liu, A. Liashenko, P. Piskorz, I. Komaromi, R. Gomperts, R.L. Martin, D.J. Fox, T. Keith, M.A. Al-Laham, C.Y. Peng, A. Nanayakkara, C. Gonzalez, M. Challacombe, P.M.W. Gill, B. Johnson, W. Chen, M.W. Wong, J.L. Andres, C. Gonzalez, M. Head-Gordon, E.S. Replogle, J.A. Pople, Gaussian, Inc., Pittsburgh PA, 1998
21. Ö. Farkas, S.J. Salpietro, P. Császár, I.G. Csizmadia, J. Mol. Struct. (Theochem) **367**, 25 (1996)
22. W. Viviani, J.-L. Rivail, A. Perczel, I. Csizmadia, J. Am. Chem. Soc. **115**, 8321 (1993)
23. M. McAllister, G. Endredi, W. Viviani, A. Perczel, P. Császár, J. Ladik, J.-L. Rivail, I. Csizmadia, Can. J. Chem. **73**, 563 (1995)
24. R. Bader, in *Atoms in Molecules: a Quantum Theory* (Clarendon Press, Oxford, 1990)
25. R. Bader, J. Phys. Chem. A **102**, 7314 (1998)
26. (a) D. Whiterfield, T. Tang, J. Am. Chem. Soc. **115**, 9648 (1993); (b) U. Koch, P. Popelier, J. Phys. Chem. **99**, 9747 (1995); (c) D. Whitefield, D. Lamba, T. Tangm, I. Csizmadia, Carbohydrate Res. **286**, 17 (1996); (d) J. Platts, S. Howardm, B. Bracke, J. Am. Chem. Soc. **118**, 2726 (1996); (e) D. Fang, P. Fabian, Z. Szekely, X. Fu, T. Tang, I. Csizmadia, J. Mol. Struct. (Theochem) **427**, 243 (1998); (f) P. Popelier, J. Phys. Chem. A **102**, 1873 (1998)
27. (a) H. Baldoni, L. Torday, A. Rodríguez, G. Zamarbide, R. Enriz, C. Sosa, Ö. Farkas, I. Jákli, A. Perczel, I. Csizmadia, *5th World Congress of Theoretically Oriented Chemists (WATOC)*, Book of Abstracts (p. 212) London, 1999; (b) H. Baldoni, G. Zamarbide, R. Enriz, E. Jáuregui, Ö. Farkas, A. Perczel, S. Salpietro, I. Csizmadia, J. Mol. Struct. (Theochem) **500**, 97 (1998)
28. PC SPARTAN PRO Wavefunction, Inc., Pittsburg PA (1996-2000)
29. I. Jákli, A. Perczel, Ö. Farkas, M. Hollósi, I. Csizmadia, J. Mol. Struct. (Theochem) **455**, 303 (1998)
30. H. Baldoni, A. Rodríguez, G. Zamarbide, R. Enriz, Ö. Farkas, P. Császár, L. Torday, C. Sosa, I. Jákli, A. Perczel, M. Hollósi, I. Csizmadia, J. Mol. Struct. (Theochem) **465**, 79 (1999)
31. I. Jákli, A. Perczel, Ö. Farkas, P. Császár, C. Sosa, I. Csizmadia, J. Comp. Chem. **21**, 626 (2000)
32. M. Zamora, H. Baldoni, A. Rodríguez, R. Enriz, C. Sosa, A. Perczel, A. Kucsman, Ö. Farkas, E. Deretey, J. Vank, I. Csizmadia, Can J. Chem (in press, 2002)
33. H. Berman, J. Westbrook, Z. Feng, G. Gilliland, T. Bhat, H. Weissig, I. Shindyalov, P. Bourne, Prot. Data Bank Nucl. Acids Res. **28**, 235 (2000), last update: 26-Feb-2002